Research Article

# Experimental nerve transfer model in the neonatal rat

https://doi.org/10.4103/1673-5374.324851
Date of submission: January 17, 2021
Date of decision: February 26, 2021
Date of acceptance: March 23, 2021
Date of web publication: September 17, 2021

Matthias E. Sporer[1, 2, 3], Martin Aman[1, 3], Konstantin D. Bergmeister[1, 4], Dieter Depisch[1, 2], Katharina M. Scheuba[1], Ewald Unger[5], Bruno K. Podesser[3], Oskar C. Aszmann[1, 2, 6, *]

**Graphical Abstract** *Effects of selective nerve transfers on the immature motor unit*

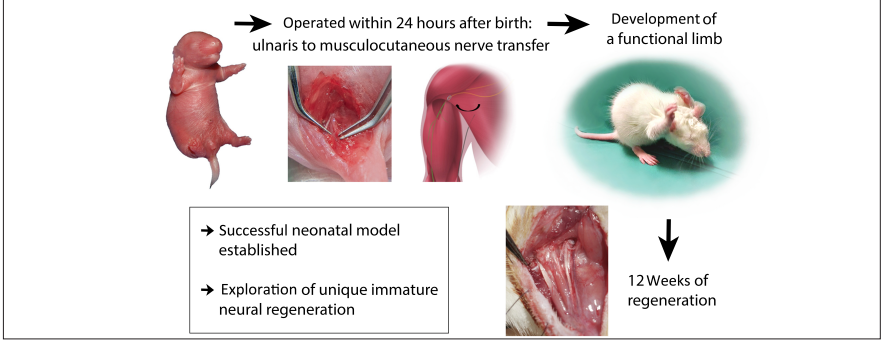


## Abstract

Clinically, peripheral nerve reconstructions in neonates are most frequently applied in brachial plexus birth injuries. Most surgical concepts, however, have investigated nerve reconstructions in adult animal models. The immature neuromuscular system reacts differently to the effects of nerve lesion and surgery and is poorly investigated due to the lack of reliable experimental models. Here, we describe an experimental forelimb model in the neonatal rat, to study these effects on both the peripheral and central nervous systems. Within 24 hours after birth, three groups were prepared: In the nerve transfer group, a lesion of the musculocutaneous nerve was reconstructed by selectively transferring the ulnar nerve. In the negative control group, the musculocutaneous nerve was divided and not reconstructed and in the positive control group, a sham surgery was performed. The animal´s ability to adapt to nerve lesions and progressive improvement over time were depict by the Bertelli test, which observes the development of grooming. Twelve weeks postoperatively, animals were fully matured and the nerve transfer successfully reinnervated their target muscles, which was indicated by muscle force, muscle weight, and cross sectional area evaluation. On the contrary, no spontaneous regeneration was found in the negative control group. In the positive control group, reference values were established. Retrograde labeling indicated that the motoneuron pool of the ulnar nerve was reduced following nerve transfer. Due to this post-axotomy motoneuron death, a diminished amount of motoneurons reinnervated the biceps muscle in the nerve transfer group, when compared to the native motoneuron pool of the musculocutaneous nerve. These findings indicate that the immature neuromuscular system behaves profoundly different than similar lesions in adult rats and explains reduced muscle force. Ultimately, pathophysiologic adaptations are inevitable. The maturing neuromuscular system, however, utilizes neonatal capacity of regeneration and seizes a variety of compensation mechanism to restore a functional extremity. The above described neonatal rat model demonstrates a constant anatomy, suitable for nerve transfers and allows all standard neuromuscular analyses. Hence, detailed investigations on the pathophysiological changes and subsequent effects of trauma on the various levels within the neuromuscular system as well as neural reorganization of the neonatal rat may be elucidated. This study was approved by the Ethics Committee of the Medical University of Vienna and the Austrian Ministry for Research and Science (BMWF-66.009/0187-WF/V/3b/2015) on March 20, 2015.

**Key Words:** brachial plexus birth injury; experimental rat model; extremity reconstruction; methodological paper; neonatal rat; nerve reconstruction; nerve regeneration; nerve transfer; neural plasticity; peripheral nerve surgery

Chinese Library Classification No. R459.9; R364; R615

## Introduction

Injuries of the immature neuromuscular system strike at a time of delicate fine-tuning between motoneuronal and muscular development. Clinically, peripheral nerve reconstructions in neonates are most frequently applied in brachial plexus birth injuries (BPBI) (Costales et al., 2019). Here, the consequences

[1]Christian Doppler Laboratory for the Restoration of Extremity Function, Department of Surgery, Medical University of Vienna, Vienna, Austria; [2]Clinical Laboratory for Bionic Extremity Reconstruction, Department of Surgery, Medical University of Vienna, Vienna, Austria; [3]Division of Biomedical Research, Medical University of Vienna, Vienna, Austria; [4]Department of Plastic, Aesthetic and Reconstructive Surgery, University Hospital of St. Poelten, Karl Landsteiner University of Health Sciences, St. Poelten, Austria; [5]Center for Medical Physics and Biomedical Engineering, Medical University of Vienna, Vienna, Austria; [6]Division of Plastic and Reconstructive Surgery, Medical University of Vienna, Vienna, Austria
***Correspondence to:** Oskar C. Aszmann, MD, PhD, oskar.aszmann@meduniwien.ac.at.
https://orcid.org/0000-0001-5530-726X (Oskar C. Aszmann)

***Funding:*** *This study was supported by the Christian Doppler Research Association and the European Research Council under the European Union's Horizon 2020 research and innovation program (both to OCA).*
***How to cite this article:*** *Sporer ME, Aman M, Bergmeister KD, Depisch D, Scheuba KM, Unger E, Podesser BK, Aszmann OC (2022) Experimental nerve transfer model in the neonatal rat. Neural Regen Res 17(5):1088-1095.*

can result in dramatic, often life-long disabilities of affected children (Malessy and Pondaag, 2009; Pondaag and Malessy, 2018). Given an incidence rate between 0.42 and 3.0 of 1000 live births (Birch, 2002; Evans-Jones et al., 2003; Malessy and Pondaag, 2009; Pondaag and Malessy, 2018) the continuous medical and social support leads to high socioeconomic costs (Brauer and Waters, 2007).

Clinical and experimental studies in adults have shown that surgical treatments not only alter the peripheral nervous system, but also change the entire motor unit from the spinal cord to the target muscle (Korak et al., 2004; Bergmeister et al., 2016a, 2019; Kapelner et al., 2016). Given that the neuromuscular system of neonates is still under structural development, clinical presentation and neural reorganization differ fundamentally from adults. Thus, these findings cannot be transferred automatically to the neonatal nervous system (Bower, 1990; Wu et al., 1995; Birch, 2002; Ochiai et al., 2002; Korak et al., 2004; Navarro et al., 2007). Due to shorter limbs with shorter regeneration distances and a tremendously adaptive central nervous system, neonates and children have a greater recovery potential (Korak et al., 2004). Other critical factors such as the time sensitive influences of growth factors (Aszmann et al., 2004; Fornaro et al., 2020), the axonal innervation density of individual muscles, as well as the cortical representation of the extremity following surgery (Schott, 1993; Farina et al., 2017; Li et al., 2021) also vary substantially.

A wealth of neonatal rat models are addressing secondary pathologies, such as joint deformities, contractures, and muscle imbalances (Kim et al., 2009; Weekley et al., 2012; Soldado et al., 2014; Nikolaou et al., 2015). Likewise, neural reorganization and spinal cord plasticity (Tada et al., 1979; Wu et al., 1995; Ochiai et al., 2002; Aszmann et al., 2004; Korak et al., 2004) following BPBI have been investigated. These models rather focus on reorganizational processes either with direct or without surgical repair. However, substantial nerve defects with a corresponding traction neuroma in BPBI allow neither direct repair nor specific restoration of the native situs, and thus neurons are surgically rerouted to novel targets. Conventional approaches to restore elbow flexion, for example, include transferring fascicles of the ulnar nerve, intercostal, or pectoral nerves to the musculocutaneous nerve (Oberlin et al., 1994; Malessy and Pondaag, 2009; Schreiber et al., 2015; Tse et al., 2015; Ray et al., 2016). Also in the event of root avulsions, axonal alignment to original targets is dramatically altered and ultimately adds to neural confusion (Birch, 2002; Korak et al., 2004; Malessy and Pondaag, 2009). Yet, the effects of selective nerve transfer (SNT) and subsequent axonal realignment in these severe nerve defects as a primary goal has never been tackled and its influence may be underestimated in neonates (Malessy and Pondaag, 2009; Tse et al., 2015). Hence, an experimental, neonatal model is needed, in which the surgical treatment of BPBI can be simulated, and the effects of neural reorganization evaluated (Navarro et al., 2007).

Here, we present a feasible, experimental forelimb model in the neonatal rat, which helps to further investigate neural reorganization after peripheral nerve reconstruction. This model describes the details of SNT in neonatal rats operated within 24 hours after birth rather than delayed repair, as common in BPBI. Still the effects on the respective target muscles but also the consequences to the immature peripheral nervous system can be investigated. Thereby, our concepts of nerve reconstruction may be improved to limit the dire sequelae of BPBI.

## Materials and Methods

### Experimental design

To test surgical feasibility, anatomical dissections were conducted bilaterally in four euthanized Sprague-Dawley neonates (Strain Code 400, Charles River Laboratories, Wilmington, MA, USA) studying the neuromuscular anatomy of the neonatal brachial plexus. To optimize *in vivo* explorations, preliminary surgical and anesthesiologic tests were conducted in eight pilot neonates. Subsequently, the core experiment was conducted in 25 neonate rats (male, 6–8 g), which were operated within 24 hours after birth (**Figure 1**). Due to three operative drop outs in the core experiment a total of 28 rats were included in this study. Littermate pups were blindly assigned to the following three groups. For the positive control group, ten animals received sham surgery with skin incision, exposure of the relevant nerves, and closure (sham group). The musculocutaneous nerve (MCN) with its targets was explored in five of these sham animals and the ulnar nerve (UN) in the remaining five. For the negative control group, the MCN was dissected and divided in five animals, but here, no reconstruction was performed. In order to guarantee better comparability, in the negative control group, the MCN was reflected back and fibrin glue was also applied. A total of ten animals underwent a SNT, as described below (nerve transfer group). All animals received humane care in compliance with the principles of laboratory animal care as recommended by Federation of European Laboratory Animal Science Associations (FELASA) (Guillen, 2012). Approval was obtained prior to the study from the ethics committee of the Medical University of Vienna and the Austrian Ministry for Research and Science (BMWF: Bundesministerium fuer Wissenschaft und Forschung, reference number: BMWF-66.009/0187-WF/V/3b/2015, approval date: March 20, 2015).

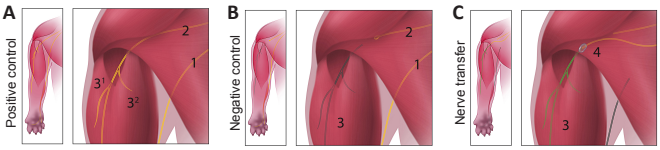


**Figure 1** | **Experimental design.**
(A) Positive control group with sham surgery (exposure of anatomical situs). (B) Negative control group with a dissected musculocutaneous nerve and no reconstruction of elbow flexion. (C) Nerve transfer group with a nerve transfer from the ulnar nerve to the musculocutaneous nerve. 1: Ulnar nerve; 2: musculocutaneous nerve; 3: biceps muscle ($3^1$: long head, $3^2$: short head); 4: nerve transfer.

### Nerve transfer surgery

Due to the diminutive anatomical proportions in the neonatal rat, the entire nerve transfer procedure was performed using an operating microscope (Zeiss S88, Zeiss, Munich, Germany) under maximal magnification (20×). Neonates were completely naked when operated within 24 hours after birth and thus the cephalic and median cubital vein were clearly visible through the skin. These provided sufficient landmarks for executing the 8–10 mm long, S-shaped skin incision. Afterwards, the subcutaneous tissue was bluntly mobilized and the pectoral muscles were carefully undermined. Through a layered incision of the pectoralis major and minor muscle, and continuous yet restrained hemostasis, the brachial plexus and its terminal branches became accessible. Direct grasping of the nerves during dissection was avoided. Then, the UN was dissected and cut distally just before entering the cubital tunnel to provide appropriate length for the SNT. When dissecting the UN, particular attention had to be paid to the vascular bundle, since even slight traction resulted in vessel damage and subsequently uncontrollable bleeding. Next, the MCN was dissected and proximally cut. Since both ends retracted, a gap of approximately 3 mm was created. To prevent spontaneous regeneration towards its original targets, the distal end of the MCN was reflected backwards (see negative control group). Consecutively, the proximal UN and distal MCN were coapted in an end-to-end fashion

without any tension at the medial bicipital sulcus lateral to the brachial artery. Since suturing was not feasible due to the size mismatch and the lack of epineurium, the nerve endings were approximated with a 2-component fibrin adhesive (Tisseel, Baxter, Frankfurt). Afterwards, the pectoralis minor and major muscle were sutured in layers by vertical mattress stitches. The skin was sutured by simple interrupted stitches using the same suture (9-0 Prolene, Ethicon, Johnson and Johnson Medical Care, Austria) (**Figures 2** and **3**).

**Anesthesia, postoperative care and euthanasia**

Preoperatively, analgesia was induced using buprenorphine (0.005 mL/g body weight, subcutaneously [s.c.], Reckitt Benckiser GmbH, Slough, UK) 1 hour before surgery. Initiation and maintenance of anesthesia was achieved with inhaled 2% isoflurane (Zoetis GmbH, Vienna, Austria), whereby oxygen content (3–5 L/min) was adapted continuously according to clinical appearance of the neonate, in order to ensure sufficient oxygenation. Since intubation was not feasible, an inhalation mask was used, and hence, spontaneous breathing was vital. For postoperative analgesia, all neonates received additional buprenorphine s.c. within 1 to 2 hours, before being returned to the dam. Drinking water of the dam was mixed with piritramide (Hameln Pharma GmbH, Hameln, Germany) and glucose (two ampules equaling 30 mg piritramide + 10 mL 10% glucose solution in 250 mL drinking water) (Danneman and Mandrell, 1997; Seitz, 2011). Postoperatively, all animals were checked daily and documented for signs of pain, wound healing disorders, or motor deficiencies. Follow-up examinations were performed under general anesthesia/analgesia via intraperitoneal injection of ketamine (100 mg/kg body weight, Ogris Pharma GmbH, Wels, Austria) and xylazin (5 mg/kg body weight, Bayer Austria GmbH, Vienna, Austria), 1.5% inhalative isoflurane (tracheal tube) and piritramide injections (piritramide 0.3 mg/kg, s.c.). Euthanasia was conducted under general anesthesia with a 1 mL intracardial injection of pentobarbital (300 mg/mL, Richter Pharma AG, Wels, Austria) after repeated control of adequate anesthesia depth.

**Behavioral assessment**

Global upper extremity function was analyzed sequentially by an adapted protocol of the Bertelli test (Bertelli and Mira, 1993). The investigation was performed blinded to the treatment groups by one trained examiner. In order to allow enough time for the development of voluntary motor function, as well as sufficient wound healing, the behavioral assessment was started 2 weeks after the primary surgery. Here, spontaneous, bilateral grooming responses were provoked by squirts of sweetened water onto the animals' snouts to functionally analyze global shoulder and elbow function. The operated forelimb was thereby compared to the contralateral healthy forelimb in each animal and between the three treatment groups. Each limb was graded at 2, 3, 4, 6 and 12 weeks postoperatively applying the following score: grade 1 (no movement or mouth), grade 2 (region below the eye), grade 3 (eye), grade 4 (front of the ears), and grade 5 (behind the ears).

**Functional muscle testing**

In order to quantify muscular reinnervation and functional recovery, maximum tetanic muscle force analyses were performed 12 weeks after the primary surgery. The nerve innervating the biceps was exposed via a Z-shaped incision from the pectoral muscles to the medial epicondyle of the humerus following blunt mobilization and dissection. In the nerve transfer and negative control group, the MCN was surgically explored in order to control for aberrant reinnervation. Next, the proximal tendon of the biceps' long head was identified, divided, folded into a tendon loop, and attached to a force transducer (BG-1000; Kulite Semiconductor Products, Leonia, NJ, USA) with 3-0 non-absorbable silk. For reproducible measurements, all animals were fixed in a supine position on a custom-made platform with the humeral head and elbow firmly secured to provide adequate stability. For the maximum tetanic muscle force analysis, the innervating nerve was hooked by a shielded bipolar silver wire cuff-electrode and then stimulated for 300 µs with 30–100 Hz and an amplitude of 2–6 V by a Grass S88 Stimulator (Grass Instrument Co., Quincy, MA, USA). Optimal muscle lengths and tension were predefined by means of individual stimulations and subsequently used for all measurements. Exsiccation was prevented by bathing exposed structures regularly in warm saline (36°C) during the entire procedure. Additionally, the procedure was paused for 3 minutes after each supramaximal stimulation to allow muscle regeneration. Five measurements were obtained, the highest and lowest value discarded and the mean calculated of the remaining three measurements. Following functional muscle testing, biceps innervating nerves were cut to survey for neurotomy reaction. Here, an immediate twitch of the biceps muscle following nerve transection was rated as an existing and functional innervation.

**Muscle analyses**

Following functional testing, the whole biceps muscle was carefully harvested, after tendons and surrounding connective tissue had been removed. Consecutively, biceps muscles were individually weighed and immediately embedded in optimal cutting temperature (OCT) compound (Tissue-Tek, Sakura Finetek, CA, USA), frozen in liquid nitrogen/cooled isopentane, and stored at –80°C for at least 24 hours. To further examine the effects of muscle de- and reinnervation, 10 µm full cross-sectional samples were taken from the midportion of the muscle, cut at –20°C with a cryotome (Leica, Nussloch, Germany), applied to Superfrost Ultra Plus slides (Thermo Fisher Scientific Menzel GmbH, Braunschweig, Germany), and prepared for staining. Afterwards, a standard Masson-Goldner-Trichrome staining (Method N° HT15, Sigma-Aldrich Handels GmbH, Vienna, Austria) was applied. Whole cross sections of biceps muscle images were acquired by transmitted-light microscopy using a fully integrated imaging system (TissueFAXS, Tissuegnostics, Austria), exported as TIF files and assessed by ImageJ (NIH, Bethesda, MD, USA) (Schindelin et al., 2012). Finally, the cross sectional area of the eutrophic biceps muscle excluding muscle fibrosis was measured.

**Retrograde labeling**

The effect of nerve transfers on the spinal cord was assessed by quantitative analyses of motoneurons using retrograde labeling. In nine experimental animals, the transferred nerve was labeled 12 weeks after the nerve transfer distal to the coaptation site just before entering the biceps muscle. In order to establish a baseline for comparison, the number of motoneurons innervating the MCN and UN were analyzed. The MCN was cut before entering the biceps muscle in five control animals, natively labeled and quantified. In the five remaining sham animals, the UN was cut at two-thirds of the humerus and its native motoneuron pool explored. In all groups, motoneurons were labeled using 10% Fluoro Ruby (Alexa Fluor 555 Dye, Thermo Fischer Scientific, Waltham, MA, USA), as previously described (Hayashi et al., 2007). In brief, the nerves were stained for 60 minutes in a well filled with retrograde tracer. After six days of retrograde dye transport to the spinal cord, animals were deeply anesthetized, followed by a left ventricular perfusion with 200 mL of warmed PBS and afterward 400 mL of 4% paraformaldehyde in PBS. Then, the spinal cord segments C4-T2 were harvested, stored in 4% paraformaldehyde for 24 hours, postfixed with 30% sucrose, and finally embedded in Tissue-Tek. The spinal cord was cut into 50 µm longitudinal sections using a cryostat (Leica). In each spinal cord section, the number of labeled motor cell

bodies was quantified under a fluorescence microscope (Zeiss Axio Imager 2) at 20× magnification. Quantification was done by one trained observer blinded to all groups. For the motoneuron analysis, the total amount of retrograde labeled neurons of the ventral horn of the spinal cord with a distinct nucleus were quantified.

### Statistical analysis

Statistical analyses were done with SPSS (V.21, IBM, Armonk, NY, USA). First, normal distribution of all data were analyzed and verified graphically by using box plots, as well as by the Kolmogorov-Smirnov test. All presented data are reported as mean values and corresponding standard deviation. Subsequently, the statistical evaluation was carried out by an independent samples *t*-test for metric and a one-way analysis of variance (ANOVA) with a *post hoc* Tukey's test for interval scaled data. *P* values less than 0.05 were considered statistically significant, and *P* values less than 0.01 as highly significant. Correlation analyses were calculated using a Pearson's correlation coefficient.

## Results

### Surgical anatomy in the neonatal rat-model

Prior to the core experiment, brachial plexus anatomy was bilaterally explored in four euthanized animals and a selective nerve transfer was found to be surgically feasible. The neonatal brachial plexus and its terminal branches were analogous to human anatomy. However, when operating within 24 hours after birth, not only neural but also muscular and connective tissue were still indiscriminate and of high plasticity (**Figure 2**). Hence, the procedure and the perioperative management had to be iteratively optimized in eight pilot neonates.

Due to their easy ventral accessibility, the median and ulnar nerve presented as potential donor nerves. However, the overall motor and sensory deficit in the palm was considered to be more limiting when sacrificing the median nerve. Furthermore, the UN has a perfectly branchless course running at first anteromedially to the brachial artery in the medial bicipital sulcus and finally passing behind the medial epicondyle in the cubital tunnel. Thus, the UN could easily be dissected far enough to obtain a sufficient length for a tension free nerve transfer to the MCN (**Figure 2**). In the euthanized and pilot animals, the dissectible length of the UN measured 2.1 ± 0.3 mm depending mostly on the course of the vascular bundle. Even though its efferent and afferent innervation pattern is analogous to human, the loss of the entire ulnar function was not found to be critical in the rat and notably did not lead to automutilation of the rat´s paw. The MCN was chosen as recipient nerve, with regard to the high clinical relevance of elbow reanimation and the fact that a similar nerve transfer (Oberlin transfer) is among the most widely used in upper brachial plexus injuries (Oberlin et al., 1994; Schreiber et al., 2015).

### Nerve transfer surgery in the neonatal rat-model

In five out of eight pilot animals the nerve transfer surgery was performed successfully, and the initial operation was survived (drop out = 37.5%). In the core experiment ($n$ = 28) mean operative complication rate decreased from 14% ($n$ = 2 out of 14) in the first half of operated animals to 7% in the second ($n$ = 1 out of 14). The overall drop-out rate was statistically significantly reduced over the course of the experiment ($P < 0.001$). Summarized, in six animals intraoperative fatal complications were documented. Intraoperative fatal complications resulted from anesthesia difficulties, arterial or venous bleeding. Anesthesia difficulties ($n$ = 3) were accompanied by complete respiratory arrest. Following arterial injury ($n$ = 2) and the corresponding blood loss, death was imminent. One animal died within twelve hours postoperatively due to continuous venous bleeding ($n$ = 1). In the core experiment, mean time between skin incision and closure of the nerve transfer surgeries was 33.5 ± 5.3 minutes. Postoperatively, neonates showed no signs of pain or distress under the given pain medication scheme and wound healing was uneventful (**Figure 3**).

### Behavioral testing and development

Compared to the contralateral side, an impaired and delayed development of the operated extremity was evident in the nerve transfer group for about 20 days. Here, simple movements were restricted and the development of a stable gait was delayed. These limitations were evident in the negative control group for about 6 weeks and were not found in sham animals. The regenerative process was also apparent in the Bertelli Test. Here animals in the negative control and nerve transfer groups achieved scores of 1.5 ± 0.5 and 1.4 ± 0.5, respectively, at the age of 2 weeks ($P = 0.949$). This resulted from both initially being unable to flex their elbow sufficiently. Even though the sham group only achieved 3 ± 0.7 out of 5 points at the same age, the difference was statistically significant compared with the transfer animals ($P < 0.001$; **Figure 4**). However, this deficit recovered continuously and faster over the following weeks in the nerve transfer group than in the negative control (Supplementary Video). Six weeks postoperatively, there was no statistically significant difference found between the sham (5 ± 0) and nerve transfer group (4.8 ± 0.4; $P = 0.382$). At this age, the negative control group only achieved 3.8 ± 0.4, which was significantly lower than in the nerve transfer group ($P < 0.001$). After 12 weeks, nerve transfer and sham animals both were all able to reach behind the ears and, thus, scored the maximum of five points. The negative control animals never achieved this grade of recovery (4 ± 0; **Figure 4**).

Finally, over the entire course of this study, neither automutilation nor a noticeable, perpetual disuse of the operated limb, were detected in any experimental animal. At the age of 12 weeks, animals weighed 406.6 ± 31.8, 396.4 ± 27.4, and 410.8 ± 34.8 g in the positive, negative, and nerve transfer groups, respectively. Here, no statistically significant difference was found between the nerve transfer and both control groups ($P = 0.791$ and $P = 0.435$).

### Macroscopic examination, functional muscle testing and muscle analyses

Detailed inspection during dissection showed mild hypertrophy of the radial muscles of the forearm, the pectoralis major and minor muscle in both, the nerve transfer and negative control group. In these groups, the MCN was macroscopically not identifiable at the brachial plexus level, as it appeared to be completely degenerated. In the negative control group, neither dissection, muscle force analysis, nor histologic muscle assessment indicated any signs of reinnervation of the transected MCN towards its original targets. The fibrin matrix itself was not found to facilitate any neural regeneration.

Extremity function was evaluated by maximum tetanic muscle force analysis of the biceps' long head (MF), neurotomy reaction during muscle harvest, as well as muscle weight (MW) and cross-sectional area of the eutrophic biceps muscle (MA) (**Figure 5**). Following 12 weeks of nerve regeneration, the nerve transfer group achieved a MF of 1.08 ± 0.38 N. In contrast, the mean value in the sham group was 3.14 ± 0.39 N and in the negative control group, no muscle contraction was excitable to any extent. The difference between the nerve transfer and the negative control was statistically significant ($P < 0.001$); as well as the difference between the nerve transfer and the sham group ($P < 0.001$). By applying a Masson-

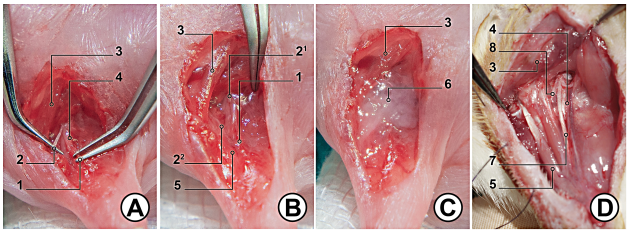


**Figure 2 | Surgical anatomy in the neonatal rat.**
(A) Operation situs before the nerve transfer. Especially note the highly plastic and indiscriminate tissue. (B) Selective nerve transfer: The ulnar donor nerve is transferred to the musculocutaneous nerve to restore elbow flexion. Neural confusion is provoked to evaluate neural plasticity. (C) As suturing was not feasible, the nerve endings were connected with a 2-component fibrin adhesive. (D) Nerve transfer after 12 weeks. 1: Ulnar nerve; 2: musculocutaneous nerve ($2^1$ proximal, $2^2$ distal); 3: pectoral muscles; 4: brachial artery; 5: biceps muscle; 6: fibrin glue; 7: median nerve; 8: nerve transfer.

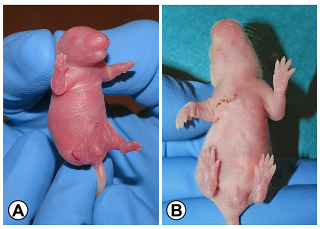


**Figure 3 | Nerve transfer surgery in the neonatal rat.**
(A) Male neonatal rat before surgery at the age of 20 hours. Note the transparent skin and the still undeveloped anatomical structures (hands, eyes and ears). (B) Rat at the age of 1 week after nerve transfer surgery. Especially note the healed, infraclavicular incision and the paralysis of the right extremity at that time.

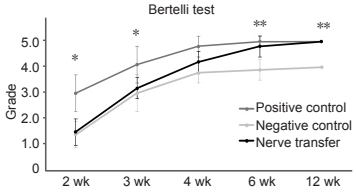


**Figure 4 | Regenerative process in the Bertelli test.**
At the age of 2 weeks, neonates do not achieve full score, which is indicated by the sham group. Within the first four weeks after birth, the grooming response fully develops. The negative control ($n$ = 5) and nerve transfer group ($n$ = 10) were initially unable to flex their elbow sufficiently. In the nerve transfer group, this deficit fully recovered over the following weeks. Even though biceps function was not restored in the negative control group, they achieved a satisfying grooming response. The trend of the positive control group ($n$ = 10) depicts the development of grooming within the first weeks after birth in neonatal rats. The Y-axis indicates functional regeneration of global shoulder and elbow funciton, assessed by the Bertelli test (Bertelli and Mira, 1993). Here, the grooming response is differentiated from grade 1 (no movement or mouth), to grade 2 (region below the eye), grade 3 (eye), grade 4 (front of the ears), and grade 5 (behind the ears). Values are presented as mean and standard deviation. * Significant difference between nerve transfer and positive control group ($P$ < 0.001). ** Significant difference between nerve transfer and negative control group ($P$ < 0.001). One-way analysis of variance with *post hoc* Tukey's test was used.

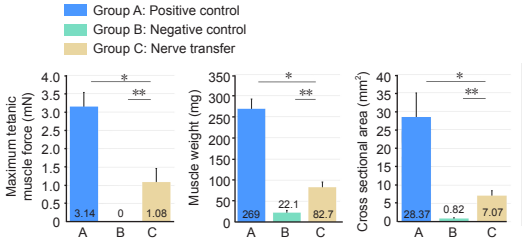


**Figure 5 | Functional muscle testing and muscle analyses.**
Following completed nerve regeneration, functional muscle testing and evaluation of the biceps's long head demonstrated successful reinnervation in all nerve transfer animals ($n$ = 10). Comparing the nerve transfer to the negative control group ($n$ = 5), a statistically significant difference was found in maximum tetanic muscle force, muscle weight and cross sectional area analyses (independent samples $t$-test, **$P$ < 0.001). Especially note that in the negative control group, no muscle contraction was excitable to any extent. However, the nerve transfer group did not completely achieve the values in the sham group (independent samples $t$-test, *$P$ < 0.001). A high Pearson correlation coefficient was found between cross sectional muscle area and muscle weight ($r$ = 0.96, $P$ > 0.01)), but also cross sectional muscle area and maximum tetanic muscle force ($r$ = 0.94, $P$ > 0.01). Values are presented as mean and standard deviation.

Goldner-Trichrome staining, eutrophic muscle fibers were distinguished from muscle fibrosis. In the negative control, endo- and perimysial fibrosis, along with fatty degeneration, decreased myofiber diameter, and degenerated, atrophic muscle fibers were observed (**Figure 6**). In this group, the remaining hypotrophic MA measured 0.82 ± 0.28 $mm^2$. In the nerve transfer group, fibrotic processes were partially observed and MA reduced accordingly. MA measured 7.07 ± 1.4 $mm^2$ in the transfer ($n$ = 8), and 28.37 ± 6.62 $mm^2$ in the sham group. The differences found in MA were statistically significant between the nerve transfer and both control groups ($P$ < 0.001 and $P$ < 0.001). The MW totaled 83.7 ± 12.3, 269.0 ± 23.2, and 22.1 ± 5.9 mg in the nerve transfer, sham and negative control groups, respectively. The MW again significantly differed between the nerve transfer and both control groups ($P$ < 0.001 and $P$ < 0.001) (**Figure 5** and **6**).

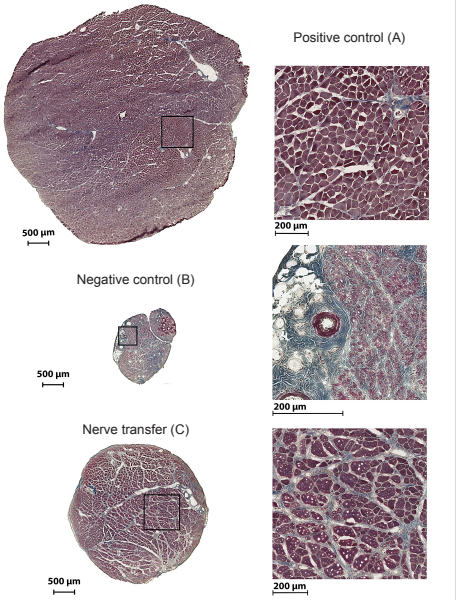


**Figure 6 | Histological muscle assessment.**
To examine the effects of muscle de- and reinnervation, cross-sectional-areas of biceps muscle were evaluated. Especially note the typical signs of muscular denervation in the negative control group: endo- and perimysial fibrosis, fatty degeneration, decreased myofiber diameter and number. The biceps muscle was reinnervated in the nerve transfer group. However, it remains histologically altered. The enlarged details of each group on the right side are marked in the respective muscle on the left side by squares. (10 µm cross-sectional muscle samples, Masson-Goldner-Trichrome staining, transmitted-light microscopy with TissueFAXS imaging system, 10× magnification). By applying a Masson-Goldner-Trichrome staining eutrophic muscle fibers can be distinguished from muscle fibrosis. Apart from the fibrosis grade, these results do not allow more precise conclusions on the changes on a muscular level.

The correlation between MA and MW as well as MA and MF was very high at 0.96 ($P$ < 0.001) and 0.94 ($P$ < 0.001) respectively, as indicated by Pearson correlation coefficient.

## Motoneuron analysis

Motoneurons were consistently located in coherent motoneuron pools of the dorsolateral region of the ventral horn. In the nerve transfer group, all motoneurons were identified in the ventral roots of the spinal nerves C8 and Th1. Following the nerve transfer within 24 hours after birth, 77.56 ± 14.96 motoneurons of the UN survived and regenerated for twelve weeks (**Figure 7**). The native UN was retrogradely labeled and contained 278.8 ± 19.89 motoneurons. This difference was statically significant ($P$ < 0.001) and the ratio of counted motoneurons corresponded to a 74% decline. Natively, the MCN contained 330.4 ± 36.75 motoneurons, inter alia originally innervating the evaluated biceps muscle. Compared with the nerve transfer group, a statically significant difference ($P$ < 0.001) was found (**Figure 7**).

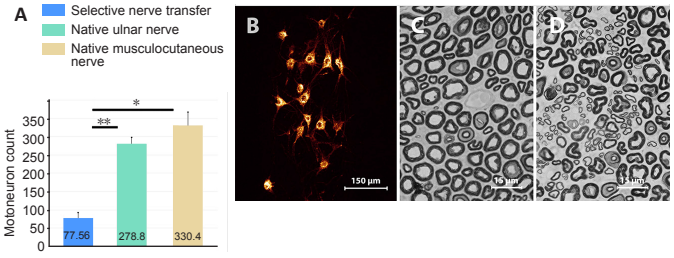


**Figure 7** | **Motoneuron analysis of the spinal cord.**
(A) The musculocutaneous and ulnar nerve were retrograde labeled and natively contained 330.4 ± 36.75 ($n$ = 5) and 278.8 ± 19.89 ($n$ = 5) motoneurons, respectively. After transferring the ulnar nerve within 24 hours after birth, due to post-axotomy motoneuron death, only 77.56 ± 14.96 ($n$ = 9) motoneurons survive for 12 weeks. Values are presented as mean and standard deviation (independent samples $t$-test, *$P$ < 0.001, **$P$ < 0.001). (B) Spinal cord photographed at the level of C5 following retrograde labeling. First, the retrograde dye (Fluoro-Ruby) is transported to the spinal cord. Consecutively, the corresponding motoneurons of an individual peripheral nerve fluoresce and can be detected as shown above. Here, the musculocutaneous nerve's motor neuron column of a sham rat is depicted and shows a coherent motoneuron pool in the dorsolateral region of the ventral horn (longitudinal section, confocal microscope, 10× magnification). (C, D) Semi-thin cross sections of the ulnar nerve harvested in pilot animals. The native ulnar nerve structure (C) can be compared to the selectively transferred ulnar nerve, taken directly at the coaptation site (D). Especially note the morphologic differences. Following nerve transfer, multiple pathologies, like thinly myelinated and dystrophic axons, but also small diameter axons, are found (staining with Osmiumtetroxid and 1,4-phenylendiamin, optical microscope, 60× magnification).

## Discussion

Apart from peripheral nerve tumors, such as neurofibromas or schwannomas and infrequent entrapment neuropathies, mainly traumatic nerve injuries are clinically relevant in newborns (Costales et al., 2019). These traumatic injuries largely occur in BPBI and a wealth of corresponding neonatal rat models have been described to investigate the devastating clinical scenario (Tada et al., 1979; Wu et al., 1995; Ochiai et al., 2002; Aszmann et al., 2004; Korak et al., 2004; Kim et al., 2009; Weekley et al., 2012; Soldado et al., 2014; Nikolaou et al., 2015). Some authors applied a nerve crush injury, others a neurotomy with direct repair, yet, no reviewed BPBI model has been devised to specifically study the effects of nerve transfer in this fragile biological period. However, today nerve transfers are an integral part in the treatment of babies suffering from BPBI (Malessy and Pondaag, 2009; Tse et al., 2015; Ray et al., 2016; Pondaag and Malessy, 2018). Additionally, axonal alignment is fundamentally altered in conventional BPBI reconstructions, when for example neurons need to be rerouted in the presence of root avulsions. We seek to fill this knowledge gap by providing an adequate and reproducible neonatal rat model.

As presented earlier in the adult model (Bergmeister et al., 2016a), also the neonatal brachial plexus and its terminal branches were identified analogous to human anatomy. In general, the similarity of the human´s and the rat´s brachial plexus makes the rat a useful experimental model (Bergmeister et al., 2016a). Even though rats use their forelimbs for feeding and grooming, findings in the forelimb of a quadruped must be considered with caution. Since the diminutive anatomical proportions of the neonatal rat did not allow nerve reconstruction in the supraclavicular region of the brachial plexus, a distal nerve transfer was executed in our study. While clinical scenarios are not identically reproduced in this manner, motoneurons are ultimately realigned in the presented model, affecting the entire transferred motor unit (Bergmeister et al., 2016a, 2019).

We found that any kind of vessel violation must be avoided, as only very little blood loss is tolerated. In the event of bleeding neither hemostasis by bipolar coagulation nor prompt treatment with fibrin glue was effective. Furthermore, nerves had to be dissected using a no-touch technique, as epineurial grasping was not feasible and axonal damage is easily provoked. When a nerve is crushed, myelin and axonal material is displaced into adjacent properties of the nerve. Continuity across the compressed region is merely maintained by the collagen fibrils of the epi-, peri-, and endoneurium, as well as the basement membranes of Schwann cells (Haftek and Thomas, 1968). Under maximal magnification of the operating microscope, unintended nerve crushes became observable and presented a prompt marker for axonal damage. Another major obstacle was adequate anesthesia of neonatal rats. In this study three neonates died of respiratory depression, presumably caused by the synergistic, cumulative effects of Buprenorphine, Isoflurane and their derivatives, which cannot be metabolized effectively due to immature liver function. Hence, the administered dosage of Buprenorphine was divided in a pre- and postoperative application. Moreover, monitoring and providing adequate, continuous anesthesia depth was challenging. Unfortunately, only a few guidelines are published for neonatal anesthesia (Danneman and Mandrell, 1997; Seitz, 2011). Additionally, commonly used methods often provide inadequate anesthesia or are associated with excessively high mortality (Danneman and Mandrell, 1997). We conclude that further research effort is required in this regard. Considering these obstacles and adapting our protocol accordingly helped to significantly improve the survival rate.

An animal's ability to adapt to nerve lesions and cope with the inevitable deficits is ultimately reflected in its behavior. Following SNT, first an impaired gait and deficits in elbow flexion due to temporary denervation of the MCN were evident. Permanent deficits in delicate paw movement on account of partial loss of intrinsic muscle function (UN innervation) were observed. These deficits were not found to be critical, most likely due to the remaining sensation of the digits innervated by the median nerve and the rudimentary function of the pollex. This conclusion is reinforced by the absence of automutilation and no statistically significant difference in the body weight of fully matured animals. The operated limb was well reintegrated into the overall body scheme over the course of regeneration. This progressive improvement is also depicted in the Bertelli Test (Bertelli and Mira, 1993), as the results sequentially increased. Twelve weeks after surgery, nerve transfer animals could reach all anatomical landmarks during grooming response. However, the Bertelli test evaluates overall upper extremity function, including elbow flexion, shoulder abduction, and anteversion. Even though the biceps muscle was not reinnervated in the negative control group, these animals achieved four out of five points. Functional deficits in elbow flexion may thus be compensated by enhanced movement over adjacent joints and of strengthening synergistic muscles. This theory is emphasized by the observed hypertrophy of the pectoral and radial muscles of the forearm noted during final assessments. Additionally, it was found that neonates in general do not achieve a full score in the Bertelli test at an early age, as they acquire this motor competence only at a later time. The trend of the sham group depicts the development of grooming within the first weeks after birth in this study.

Functional muscle testing, neurotomy reaction, and muscle assessment demonstrated that the biceps muscle was successfully reinnervated by the transferred ulnar motoneurons. However, the nerve transfer group did not achieve sham group´s values in this study. This limited regeneration might result from the effects of nerve lesions on motoneurons originating in the central nervous system. The reduction of the ulnar motoneuron pool after neonatal nerve lesions indicates that a known phenomenon termed

post-axotomy motoneuron death resulted from nerve injury at this young age (Wu et al., 1995; Lauretti et al., 2009). Here, transections of peripheral nerves are consecutively followed by the death of their corresponding motoneurons, a phenomenon even more apparent when nerves are sectioned within the first days of life in proximity to their soma (Schmalbruch, 1984). This loss is described as an essential feature of any proximal nerve injury in the early postnatal period (Korak et al., 2004), caused by retrograde degeneration (Ochiai et al., 2002) and most likely derives from an absent neurotrophic support between motoneurons and their target muscles (Lowrie and Vrbova, 1992). At an early stage of development, stimulating neurotrophic support is essential for motoneuron survival (Lowrie and Vrbova, 1992; Aszmann et al., 2004; Korak et al., 2004). As motoneurons mature, they gradually lose their target-dependency and injury-induced loss is absent in mature animals. However, post-axotomy motoneuron death described in literature often resulted in greater or even complete depletion of the motoneuron pool. This might have been prevented by establishing favorable conditions for motoneuron survival in our experimental model. Firstly, the ulnar nerve was transected distally and the remaining nerve provided a sufficient length. Secondly, the coaptation site was adjacent to the motor entry point of the biceps muscle reducing regeneration distance. Thereby, fast muscular reinnervation and corresponding early neurotrophic support facilitated motoneuronal survival (Tada et al., 1979; Schmalbruch, 1984; Lowrie and Vrbova, 1992). Even though regeneration in the nerve transfer group was limited by a diminished amount of motoneurons reinnervating the biceps muscle, the neonatal capacity of regeneration overall facilitated the restoration of a functional extremity.

The absence of aberrant reinnervation in the nerve transfer group and the complete vacancy of any regeneration signs in the negative control group suggest that no spontaneous regeneration from the MCN has happened. Even though minute anatomical dissection was performed when exploring both groups, the remainder of the dissected MCN motoneurons anatomically remains unidentified. The fibrin matrix alone did not provide an adequate substrate for the regeneration of the reflected MCN fibers. It is known that transected nerves are capable of regenerating along adjacent nerves (Aszmann et al., 2003; Navarro et al., 2007). However, retrograde labeling of the transferred nerve innervating the biceps muscle in the nerve transfer group solely presented one coherent motoneuron pool in the dorsolateral region of the ventral horn. Since motoneurons of the MCN and ulnar nerve originate from different ventral roots, adjacent regeneration is at least unlikely along the transferred UN. The un-detectability of the MCN motoneurons might result from the fact that all motoneurons could have undergone post-axotomy motoneuron death due to the relative proximal axotomy and the lack of an immediate distal target (Tada et al., 1979; Lowrie and Vrbova, 1992). However, we conclude that two instead of one motoneuron population are decimated in the event of peripheral nerve injury followed by immediate transfer in neonates, which reassures that this approach should remain abolished in the clinical practise of BPBI reconstruction.

The maturing neuromuscular system utilizes neonatal capacity of regeneration in the peripheral nervous system. Here, not only the effected motor unit is restored, but a variety of potential adaptation mechanism are utilized (Korak et al., 2004; Navarro et al., 2007; Navarro, 2009; Kapelner et al., 2016; Bergmeister et al., 2019). These effects remain to be studied in detail, but they appear to occur aside from central adaptation mechanisms, like cortical reorganization, which are reviewed and discussed elsewhere (Bower, 1990; Birch, 2002; Navarro, 2009; Baldassarre et al., 2020; Li et al., 2021).

Exploration of nerve conduction pathways, generation of target muscle action potentials, as well as comparative studies of their amplitude and latency could further elucidate the pathophysiologic understanding of peripheral nerve regeneration and adaptation mechanisms (Farina et al., 2017; Bergmeister et al., 2019; Muceli et al., 2019). Since the establishment of proprioception is especially critical in the maturing somatosensory system, the authors hope that the proposed experimental model and technical guide facilitates further research in the field of sensory circuits (Leighton and Lohmann, 2016). Furthermore, the evaluation of neurotrophic factor-related gene regulation and its effects on neonatal nerve transfers might be encouraged. Analyses in this model may be limited in the early post-operative phase, but not at the typical endpoint for such studies, given that rats have matured, and are fully developed at twelve weeks. To the best of our knowledge, all standard analyses of the peripheral nerve and motor unit system are applicable. Although not reported here, histomorphometric and immunhistochemical nerve (Gesslbauer et al., 2017) and muscle stainings (Bergmeister et al., 2016b), high-density intramuscular electromyography analyses, as well as electrophysiological evaluations are feasible (Muceli et al., 2019), and have already been performed to some extent in this model.

In conclusion, this experimental forelimb model describes the details of nerve transfers in neonatal rats operated within 24 hours after birth. Here, we present a successful nerve transfer model with a detailed technical guide, furthering reproducibility and the use of animal models to study the unique physiology of an unsolved clinical problem. Applying this model, the effects of SNT on the respective target muscles, but also the consequences to the immature motoneuron originating in the central nervous system may be studied. While satisfying regeneration of the selective nerve transfer was found, nerve lesions were identified to alter normal neonatal motor development fundamentally and lead to pathophysiological changes on the neuromuscular system. Hence, complete regeneration is unlikely and neural plasticity rather promotes the development of an overall superior and effective limb. The proposed experimental model facilitates detailed investigation of the denervation and reinnervation process in neonates with standard neuromuscular and neurotrophic factor-related analyses. Thereby, the pathophysiological understanding of BPBI may be further increased and the surgical armamentarium expanded.

**Author contributions:** *MES, OCA and KDB designed the concept of the study. MES, MA, DD, KMS and EU conducted the experiments. MES, DD and KMS performed the data acquisition and analysis. MES, KDB, MA and OCA drafted the main manuscript. Artistic conception of figures was contributed by MES. All authors contributed their specific expertise, revised any part of the work critically and approved the final version of the manuscript.*

**Conflicts of interest:** *The authors declare that they have no competing interests that might be perceived to influence the results and/or discussion reported in this paper. The authors further declare that the study was conducted in the absence of any commercial or financial relationships. Moreover, the authors disclose any conflict of interest with any products mentioned in the manuscript or competing with those.*

**Financial support:** *This study was supported by the Christian Doppler Research Association and the European Research Council under the European Union's Horizon 2020 research and innovation program (both to OCA). The funders had no role in study design, data collection and analysis, decision to publish, or preparation of the manuscript.*

**Institutional review board statement:** *The experiments were approved by the ethics committee of the Medical University of Vienna and the Austrian Ministry for Research and Science (BMWF-66.009/0187-WF/V/3b/2015) on March 20, 2015.*

**Author statement:** *The abstract has been presented at the 8th Meeting of the EURAPS Research Council (ERC), Helsinki on May 23, 2019 and the 10th Congress of World Society for Reconstructive Microsurgery (WSRM), Bologna on June 13, 2019.*

**Data sharing statement:** *Datasets analyzed during the current study are available from the corresponding author on reasonable request.*
**Plagiarism check:** *Checked twice by iThenticate.*
**Peer review:** *Externally peer reviewed.*

**Additional file:**
***Additional Video 1:*** *Bertelli test of a 4-week-old experimental rat. The shown animal underwent nerve transfer surgery of the right upper extremity within 24 hours after birth. Following four weeks of nerve regeneration spontaneous, bilateral grooming responses were provoked by squirts of sweetened water onto the animals' snouts. In this video segment, the animal achieves 4 out of 5 points since, elbow flexion is not yet fully restored at this age, but the rat already manages to reach the front of its ear on the operated side.*

## References

Aszmann OC, Winkler T, Korak K, Lassmann H, Frey M (2004) The influence of GDNF on the timecourse and extent of motoneuron loss in the cervical spinal cord after brachial plexus injury in the neonate. Neurol Res 26:211-217.
Aszmann OC, Korak KJ, Rab M, Grünbeck M, Lassmann H, Frey M (2003) Neuroma prevention by end-to-side neurorraphy: an experimental study in rats. J Hand Surg Am 28:1022-1028.
Baldassarre BM, Lavorato A, Titolo P, Colonna MR, Vincitorio F, Colzani G, Garbossa D, Battiston B (2020) Principles of cortical plasticity in peripheral nerve surgery. Surg Technol Int 36:444-452.
Bergmeister KD, Aman M, Riedl O, Manzano-Szalai K, Sporer ME, Salminger S, Aszmann OC (2016a) Experimental nerve transfer model in the rat forelimb. Eur Surg 48:334-341.
Bergmeister KD, Groger M, Aman M, Willensdorfer A, Manzano-Szalai K, Salminger S, Aszmann OC (2016b) Automated muscle fiber type population analysis with ImageJ of whole rat muscles using rapid myosin heavy chain immunohistochemistry. Muscle Nerve 54:292-299.
Bergmeister KD, Aman M, Muceli S, Vujaklija I, Manzano-Szalai K, Unger E, Byrne RA, Scheinecker C, Riedl O, Salminger S, Frommlet F, Borschel GH, Farina D, Aszmann OC (2019) Peripheral nerve transfers change target muscle structure and function. Sci Adv 5:eaau2956.
Bertelli JA, Mira JC (1993) Behavioral evaluating methods in the objective clinical assessment of motor function after experimental brachial plexus reconstruction in the rat. J Neurosci Methods 46:203-208..
Birch R (2002) Obstetric brachial plexus palsy. J Hand Surg Br 27:3-8.
Bower AJ (1990) Plasticity in the adult and neonatal central nervous system. Br J Neurosurg 4:253-264.
Brauer CA, Waters PM (2007) An economic analysis of the timing of microsurgical reconstruction in brachial plexus birth palsy. J Bone Joint Surg Am 89:970-978.
Costales JR, Socolovsky M, Sánchez Lázaro JA, Álvarez García R (2019) Peripheral nerve injuries in the pediatric population: a review of the literature. Part I: traumatic nerve injuries. Childs Nerv Syst 35:29-35.
Danneman PJ, Mandrell TD (1997) Evaluation of five agents/methods for anesthesia of neonatal rats. Lab Anim Sci 47:386-395.
Evans-Jones G, Kay SP, Weindling AM, Cranny G, Ward A, Bradshaw A, Hernon C (2003) Congenital brachial palsy: incidence, causes, and outcome in the United Kingdom and Republic of Ireland. Arch Dis Child Fetal Neonatal Ed 88:F185-189.
Farina D, Castronovo AM, Vujaklija I, Sturma A, Salminger S, Hofer C, Aszmann O (2017) Common synaptic input to motor neurons and neural drive to targeted reinnervated muscles. J Neurosci 37:11285-11292.
Fornaro M, Giovannelli A, Foggetti A, Muratori L, Geuna S, Novajra G, Perroteau I (2020) Role of neurotrophic factors in enhancing linear axonal growth of ganglionic sensory neurons in vitro. Neural Regen Res 15:1732-1739.
Gesslbauer B, Hruby LA, Roche AD, Farina D, Blumer R, Aszmann OC (2017) Axonal components of nerves innervating the human arm. Ann Neurol 82:396-408.
Guillen J (2012) FELASA guidelines and recommendations. J Am Assoc Lab Anim Sci 51:311-321.
Haftek J, Thomas PK (1968) Electron-microscope observations on the effects of localized crush injuries on the connective tissues of peripheral nerve. J Anat 103(Pt 2):233-243.
Hayashi A, Moradzadeh A, Hunter DA, Kawamura DH, Puppala VK, Tung TH, Mackinnon SE, Myckatyn TM (2007) Retrograde labeling in peripheral nerve research: it is not all black and white. J Reconstr Microsurg 23:381-389.
Kapelner T, Jiang N, Holobar A, Vujaklija I, Roche AD, Farina D, Aszmann OC (2016) Motor unit characteristics after targeted muscle reinnervation. PLoS One 11:e0149772.
Kim HM, Galatz LM, Patel N, Das R, Thomopoulos S (2009) Recovery potential after postnatal shoulder paralysis. An animal model of neonatal brachial plexus palsy. J Bone Joint Surg Am 91:879-891.
Korak KJ, Tam SL, Gordon T, Frey M, Aszmann OC (2004) Changes in spinal cord architecture after brachial plexus injury in the newborn. Brain 127:1488-1495.
Lauretti L, Pallini R, Romani R, Di Rocco F, Ciampini A, Gangitano C, Del Fa A, Fernandez E (2009) Lower trunk of brachial plexus injury in the neonate rat: effects of timing repair. Neurol Res 31:518-527.
Leighton AH, Lohmann C (2016) The wiring of developing sensory circuits—From patterned spontaneous activity to synaptic plasticity mechanisms. Front Neural Circuits 10:71.
Li C, Liu SY, Pi W, Zhang PX (2021) Cortical plasticity and nerve regeneration after peripheral nerve injury. Neural Regen Res 16:1518-1523.
Lowrie MB, Vrbova G (1992) Dependence of postnatal motoneurones on their targets: review and hypothesis. Trends Neurosci 15:80-84.
Malessy MJ, Pondaag W (2009) Obstetric brachial plexus injuries. Neurosurg Clin N Am 20:1-14, v.
Muceli S, Bergmeister KD, Hoffmann KP, Aman M, Vukajlija I, Aszmann OC, Farina D (2019) Decoding motor neuron activity from epimysial thin-film electrode recordings following targeted muscle reinnervation. J Neural Eng 16:016010.
Navarro X (2009) Chapter 27 Neural plasticity after nerve injury and regeneration. In: International Review of Neurobiology (Stefano G, Pierluigi T, Bruno B, eds), pp 483-505. San Diego, CA: Academic Press.
Navarro X, Vivo M, Valero-Cabre A (2007) Neural plasticity after peripheral nerve injury and regeneration. Prog Neurobiol 82:163-201.
Nikolaou S, Hu L, Cornwall R (2015) Afferent innervation, muscle spindles, and contractures following neonatal brachial plexus injury in a mouse model. J Hand Surg Am 40:2007-2016.
Oberlin C, Beal D, Leechavengvongs S, Salon A, Dauge MC, Sarcy JJ (1994) Nerve transfer to biceps muscle using a part of ulnar nerve for C5-C6 avulsion of the brachial plexus: anatomical study and report of four cases. J Hand Surg Am 19:232-237.
Ochiai H, Ikeda T, Mishima K, Yoshikawa T, Aoo N, Iwasaki K, Fujiwara M, Ikenoue T, Nakano S, Wakisaka S (2002) Development of a novel experimental rat model for neonatal pre-ganglionic upper brachial plexus injury. J Neurosci Methods 119:51-57.
Pondaag W, Malessy MJA (2018) Outcome assessment for Brachial Plexus birth injury. Results from the iPluto world-wide consensus survey. J Orthop Res 36:2533-2541.
Ray WZ, Chang J, Hawasli A, Wilson TJ, Yang L (2016) Motor nerve transfers: a comprehensive review. Neurosurgery 78:1-26.
Schindelin J, Arganda-Carreras I, Frise E, Kaynig V, Longair M, Pietzsch T, Preibisch S, Rueden C, Saalfeld S, Schmid B, Tinevez JY, White DJ, Hartenstein V, Eliceiri K, Tomancak P, Cardona A (2012) Fiji: an open-source platform for biological-image analysis. Nat Methods 9:676-682.
Schmalbruch H (1984) Motoneuron death after sciatic nerve section in newborn rats. J Comp Neurol 224:252-258.
Schott GD (1993) Penfield's homunculus: a note on cerebral cartography. J Neurol Neurosurg Psychiatry 56:329-333.
Schreiber JJ, Byun DJ, Khair MM, Rosenblatt L, Lee SK, Wolfe SW (2015) Optimal axon counts for brachial plexus nerve transfers to restore elbow flexion. Plast Reconstr Surg 135:135e-141e.
Seitz C (2011) Anesthesia and analgesia: Neonatal mice and rats. Boston University: Boston University- Institutional Animal Care and Use Committee.
Soldado F, Fontecha CG, Marotta M, Benito D, Casaccia M, Mascarenhas VV, Zlotolow D, Kozin SH (2014) The role of muscle imbalance in the pathogenesis of shoulder contracture after neonatal brachial plexus palsy: a study in a rat model. J Shoulder Elbow Surg 23:1003-1009.
Tada K, Ohshita S, Yonenobu K, Ono K, Satoh K, Shimizu N (1979) Experimental study of spinal nerve repair after plexus brachialis injury in newborn rats: a horseradish peroxidase study. Exp Neurol 65:301-314.
Tse R, Kozin SH, Malessy MJ, Clarke HM (2015) International Federation of Societies for Surgery of the Hand Committee report: the role of nerve transfers in the treatment of neonatal brachial plexus palsy. J Hand Surg Am 40:1246-1259.
Weekley H, Nikolaou S, Hu L, Eismann E, Wylie C, Cornwall R (2012) The effects of denervation, reinnervation, and muscle imbalance on functional muscle length and elbow flexion contracture following neonatal brachial plexus injury. J Orthop Res 30:1335-1342.
Wu Y, Li Y, Liu H, Wu W (1995) Induction of nitric oxide synthase and motoneuron death in newborn and early postnatal rats following spinal root avulsion. Neurosci Lett 194:109-112.

*C-Editors: Zhao M, Li CH; T-Editor: Jia Y*